Microsecond Time-Scale Discrimination Among Polycytidylic Acid, Polyadenylic Acid, and Polyuridylic Acid as Homopolymers or as Segments Within Single RNA Molecules

Mark Akeson,* Daniel Branton,# John J. Kasianowicz,§ Eric Brandin,# and David W. Deamer*

*Department of Chemistry & Biochemistry, University of California, Santa Cruz, CA 95064; #Department of Molecular & Cellular Biology, Harvard University, Cambridge, MA 02138; and §Biotechnology Division, National Institute of Standards & Technology, Gaithersburg, MD 20899

ABSTRACT Single molecules of DNA or RNA can be detected as they are driven through an α-hemolysin channel by an applied electric field. During translocation, nucleotides within the polynucleotide must pass through the channel pore in sequential, single-file order because the limiting diameter of the pore can accommodate only one strand of DNA or RNA at a time. Here we demonstrate that this nanopore behaves as a detector that can rapidly discriminate between pyrimidine and purine segments along an RNA molecule. Nanopore detection and characterization of single molecules represent a new method for directly reading information encoded in linear polymers, and are critical first steps toward direct sequencing of individual DNA and RNA molecules.

INTRODUCTION

We previously showed that single-stranded DNA or RNA molecules can be detected and their lengths measured when they are driven through a nanometer-scale pore (Kasianowicz et al., 1996). The pore we used was formed by α-hemolysin, a 33-kD, 293-amino acid protein isolated from *Staphylococcus aureus*. Seven α-hemolysin monomers self-assemble in a lipid bilayer to create a channel whose pore has a limiting aperture of 1.5 nm (Song et al., 1996). A pore of this diameter would be expected to accommodate single-stranded, but not double-stranded, polynucleotides. This expectation was confirmed when single-stranded DNA was shown to pass through the pore and to block the otherwise unimpeded ionic current (Kasianowicz et al., 1996). Under the same conditions, blunt-ended double-stranded DNA had no effect on pore conductance and did not pass through the pore.

Our demonstration that a nanopore can be used to measure the length of RNA or DNA molecules (Kasianowicz et al., 1996) suggested that this approach might be used to derive a direct, high-speed read-out of linear polymer sequences encoded in single molecules. Obtaining such a read-out would, at minimum, require that the channel conductance be sensitive to its pore contents and be able to discriminate between chemically or structurally distinct segments of a polymer during translocation through the pore. Here we show that the current blockades caused by homopolymers of polycytidylic acid (poly C), polyadenylic acid (poly A), and polyuridylic acid (poly U) are readily distinguished from one another based on blockade amplitude or blockade kinetics. Furthermore, we demonstrate that a nanopore can distinguish between poly C and poly A segments within a single RNA molecule.

Received for publication 19 May 1999 and in final form 13 August 1999.

Address reprint requests to Dr. Mark Akeson, Chemistry Dept., University of Santa Cruz, Santa Cruz, CA 95064. Tel.: 831-459-5157; Fax: 831-459-5158; E-mail: makeson@chemistry.ucsc.edu.

0006-3495/99/12/3227/07 $2.00

MATERIALS AND METHODS

Formation of α-hemolysin pores in low-noise, horizontal bilayers

A horizontal bilayer apparatus was developed for our experiment (Fig. 1). This Teflon apparatus combines the advantages of a conical aperture (Wonderlin et al., 1990) with those of a horizontal bilayer (Brutyan et al., 1995). Bilayers formed across the aperture of this device exhibit high resistance (>200 GΩ), low noise (<0.6 pA RMS at 5 kHz bandwidth in whole-cell mode, 0.2 pA RMS in patch mode using an Axopatch 200B amplifier), and are stable for many hours at applied voltages up to 200 mV. In addition, the bath can be tens of microliters in volume, permitting analysis of small amounts of RNA or DNA.

To form a bilayer, the Teflon aperture was coated by applying 5 μl of a 200 μg/ml solution of diphytanoyl phosphatidylcholine in spectroscopy grade hexane, which was then evaporated using a light stream of air. Most of the experiments presented in this report used a 25-μm-diameter aperture, but we have successfully used apertures <20 μm diameter. The chambers on both sides of the aperture were subsequently filled with 70 μl of buffer composed of 1.0 M KCl and 5 mM HEPES/KOH at pH 7.5. A single 1-cm-long bristle of a 000 brush was dipped into a 3 mg/ml diphytanoyl phosphatidylcholine solution in spectroscopy-grade hexadecane, and then brushed across the aperture. A 5-mV, 60-cycle square wave was applied across the aperture between two Ag-AgCl electrodes as a seal test. After a stable bilayer was formed, 0.04 μg of α-hemolysin in 10 μl buffer was added to the *cis* side of the bilayer and 120 mV potential was applied, *cis*-side negative. Typically, a single α-hemolysin channel inserted in 10–30 min. Insertion was indicated by an abrupt current increase to ~120 pA, after which the excess α-hemolysin was removed by perfusion with 2.0 ml of fresh buffer.

Preparation of RNA

Homopolymers of poly C, poly U, and poly A (2000+ nucleotide) were purchased from Fluka (Ronkonkoma, NY). Fragments were produced by hydrolysis in alkaline buffer. For a product ranging in size from 100 to 500 nucleotides in length, 2 mg full-length RNA in 1.0 ml alkaline buffer solution (40 mM $NaHCO_3$, 60 mM Na_2CO3, pH 10.2) was incubated at

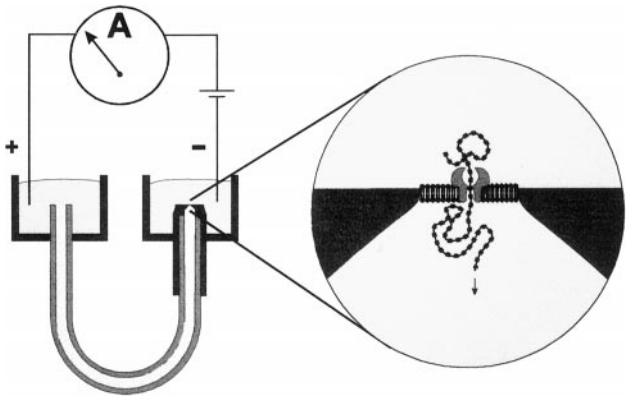

FIGURE 1 Horizontal bilayer apparatus. A U-shaped Teflon patch tube connects two 70-μl baths milled into a Teflon support (*left*). The baths and the Teflon tube are filled with 1 M KCl buffer. The baths are connected to an Axopatch 200B amplifier by Ag-AgCl electrodes. One end of the Teflon patch tube has a conical tip that narrows abruptly to a 25-μm conical aperture (*right*). Diphytanoyl phosphatidylcholine/hexadecane bilayers are formed across this aperture, and one or more α-hemolysin channels are inserted into the bilayer. Nucleic acids are driven through the α-hemolysin channel by an applied voltage of +120 mV, positive at the *trans* side.

60°C for 23.5 min. The reaction was stopped by adding 100 μl 3 M sodium acetate and 50 μl 10% glacial acetic acid. The RNA was precipitated in ethanol, re-dissolved in TE buffer, then separated by electrophoresis on an 8% polyacrylamide/TBE gel. Gel fragments corresponding to RNA of the desired lengths were then excised and the RNA eluted by electrophoresis. The sized RNA was ethanol-precipitated and re-dissolved in water or pH 7.5 TE buffer at 2–5 μg/μl.

A poly $A_{30}C_{70}$ copolymer was synthesized by in vitro transcription from a 134-base DNA oligonucleotide (TAATACGACTCACTATAGGGA $(A)_{29}(C)_{70}$GGTACCACACAC) purchased from Midland Certified Reagents (Midland, TX). Double-stranded template was synthesized from the purified single-stranded 134-mer using Sequenase (Amersham, Cleveland, OH). RNA was synthesized from this 134 nt DNA template using T7 RNA polymerase (Megashortscript, Ambion Inc., Austin, TX). After synthesis, the product was incubated at 37°C for 15 min with 2U DNAse I to remove DNA, and with 0.25 μg RNAase T1 (Life Technologies, Gaithersburg, MD) to cut off undesired ends of the RNA product 3′ to G-residues at either end of the molecule. After purification using an 8% polyacrylamide gel (1X MOPS RNA buffer, 80 V), the desired 101-nucleotide band ($A_{30}C_{70}$Gp) was excised and eluted by electrophoresis. The elution buffer was then exchanged for pH 7.5 TE buffer using a Bio-Rad 30 column (Bio-Rad, Hercules, CA).

Data acquisition and analysis

Ionic current flux through the α-hemolysin channels was measured and recorded using an Axopatch 200B integrating patch clamp amplifier (Axon Instruments, Foster City, CA) in voltage-clamp mode. Data were acquired at 10-μs intervals in the whole cell configuration and filtered at 10 kHz using a low-pass Bessel filter, or at 3-μs intervals and filtered at 100 kHz. Current blockades were examined at 120 mV (*trans*-positive). The recorded data were analyzed using pClamp6 software (Axon Instruments).

RESULTS

Analysis of poly C and poly A at 10-kHz bandwidth

Single α-hemolysin channels were introduced into high-resistance, low-noise diphytanoyl phosphatidylcholine bilayers formed across a horizontal, conical aperture at the end of a Teflon tube (Fig. 1). Single-stranded ribonucleic acid homopolymers (poly A or poly C of known lengths) were then added to the *cis* side of the bilayer and ionic current blockades were measured at 120 mV applied potential. In this and all subsequent experiments, polymer was added to the *cis* chamber to achieve concentrations between 50 and 200 μg ml^{-1}, or 4 μM for the poly A results described here. When 150 nucleotide nominal length poly A homopolymers were used, the observed blockades fell into three populations (Fig. 2 *a*): 1) relatively short (<200 μs) blockades that reduced the current to 55–65 pA of residual current (~35–50% blockades); 2) blockades of indeterminate length that reduced the current to ~55 pA (~55% blockades); and 3) blockades of 1–4 ms that reduced the current to ~20 pA (~85% blockades). We have previously shown that only the blockades that are strand length-dependent (here, the 85% blockades) represent vectorial translocation through the pore (Kasianowicz et al., 1996). The short, strand length-independent blockades of lesser amplitude (35–50% and 55% blockades), may represent collision or transient partial entry of the polymer into the α-hemolysin channel vestibule without translocation.

The pattern of blockades caused by poly C was easily distinguished from the pattern caused by poly A, whether the polymers were examined separately (Fig. 2 *b*) or in a mixture of poly C and poly A (Fig. 2 *c*). Of the blockades whose duration was strand length-dependent, poly C reduced the channel current significantly more than did poly A (~95% and 91% blockades versus ~85% blockades, respectively). Furthermore, the 95% and 91% blockades caused by poly C were shorter in duration (5 ± 2 μs per nucleotide) than were the 85% blockades caused by poly A (22 ± 6 μs per nucleotide), and poly C rarely produced the lesser amplitude blockades that were relatively common with poly A.

Comparison between poly U, poly C, and poly A at higher bandwidth

To facilitate more detailed comparisons of three different polynucleotides, subsequent data were acquired at 100-kHz bandwidth and digitally filtered as needed. When poly U blockades were compared with those caused by poly C and poly A (Fig. 3), current amplitude and blockade time together distinguished the three different polymers from each other. The current amplitude differences between poly C and poly A blockades were evident as before (Fig. 3 *a*). Although the current amplitudes of poly U blockades (18 ± 3 pA residual current) and poly A ~85% blockades (17 ± 1 pA residual current) were practically indistinguishable, the typically shorter durations of the poly U blockades were clearly distinct from those of poly A. For example, when polymers of essentially equal length were compared (175 ±

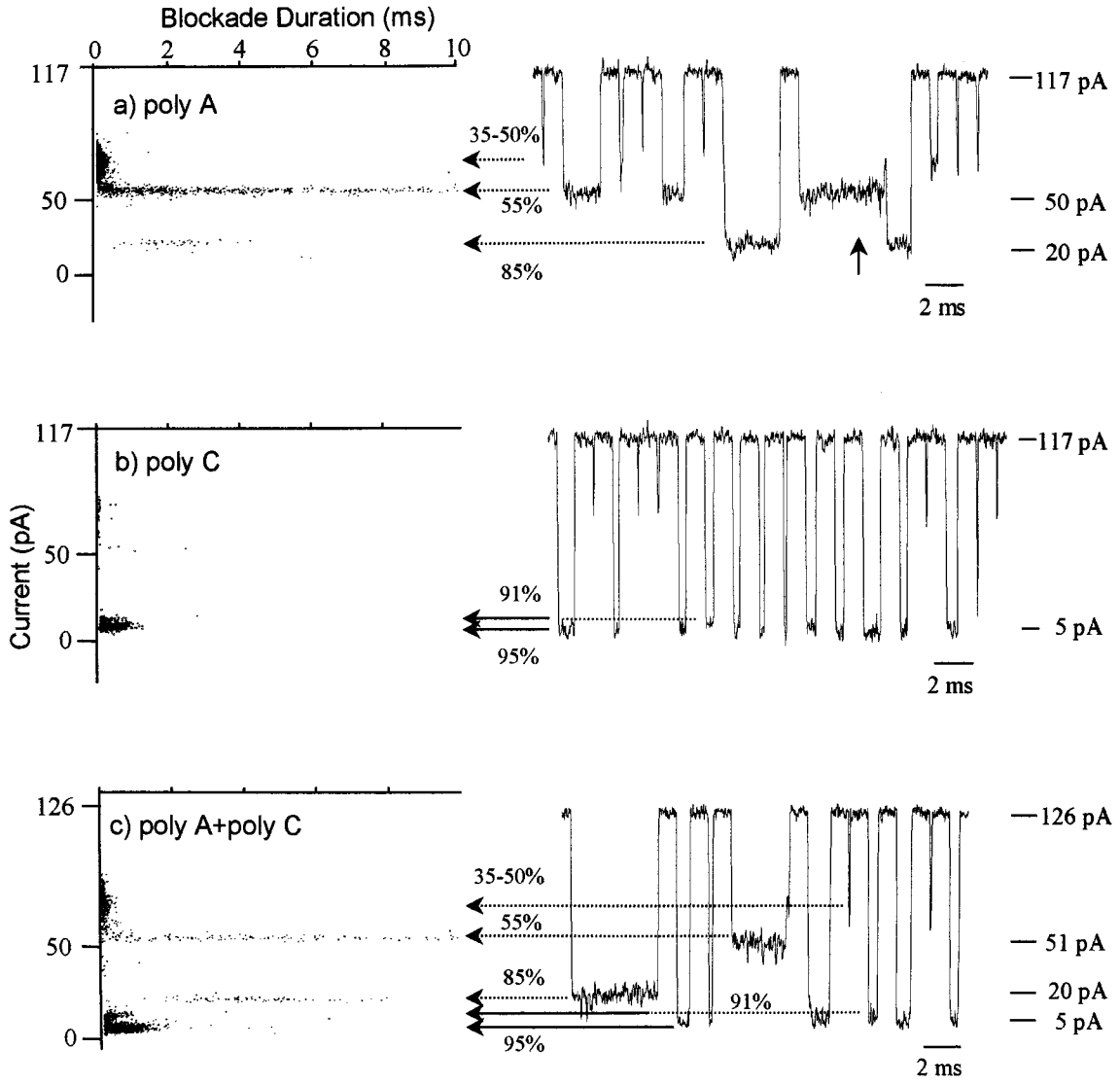

FIGURE 2 Blockades caused by RNA homopolymers. Each point in the scatter plots corresponds to the amplitude and duration of a current blockade caused by a single RNA homopolymer passing through the α-hemolysin pore. Typical blockade events from which the plots were produced are shown at right. (*a*) Blockades caused by poly A (150 nucleotide nominal length, 200 μg/ml). (*b*) Blockades of the same α-hemolysin pore caused by poly C (125 nucleotide nominal length, 200 μg/ml). (*c*) Blockades caused by a mixture of poly C (125 nucleotide nominal length) and poly A (175 nucleotide nominal length). Between experiments, small differences in the exact channel currents were caused by evaporation that increased the ionic strength of the bathing solutions (compare open channel current of 117 pA in (*a*) with open channel current of 126 pA in (*c*). The time interval between blockades was variable in these experiments. It appears to be regular because quiescent periods between events were spliced out so that numerous blockades could be presented in one figure.

50 nt poly A and 150 $\pm$ 50 nt poly U), poly A blockades were relatively long (22 $\pm$ 6 μs/nt) and commonly exhibited a shoulder at the characteristic 55% level (Figs. 2 *a* and 3 *b*). Single-level 55% blockades were also produced by poly A. Poly U blockades lacked the 55% shoulders, and were significantly shorter in duration (populations centered at 1.4 μs/nt and 6 μs/nt, Fig. 3 *b*, and Kasianowicz et al., 1996). We conclude that translocation across the α-hemolysin pore can be used to distinguish between RNA homopolymers either on the basis of blockade amplitude (poly C versus poly A or poly U), or on the basis of blockade duration and blockade pattern (poly A versus poly U).

Comparison between poly C and poly dC single-stranded DNA

As demonstrated above, poly C translocation produces distinctive 95% or 91% current blockades that are greater than blockades caused by translocation of the other RNA homopolymers. We were surprised by this result because the relatively small pyrimidines in poly C might be expected to impede ionic current less than the relatively large purines in poly A. One possible explanation is that poly C at room temperature and neutral pH conditions exists primarily as a single-stranded helix 1.3 nm in diameter (Fasman et al.,

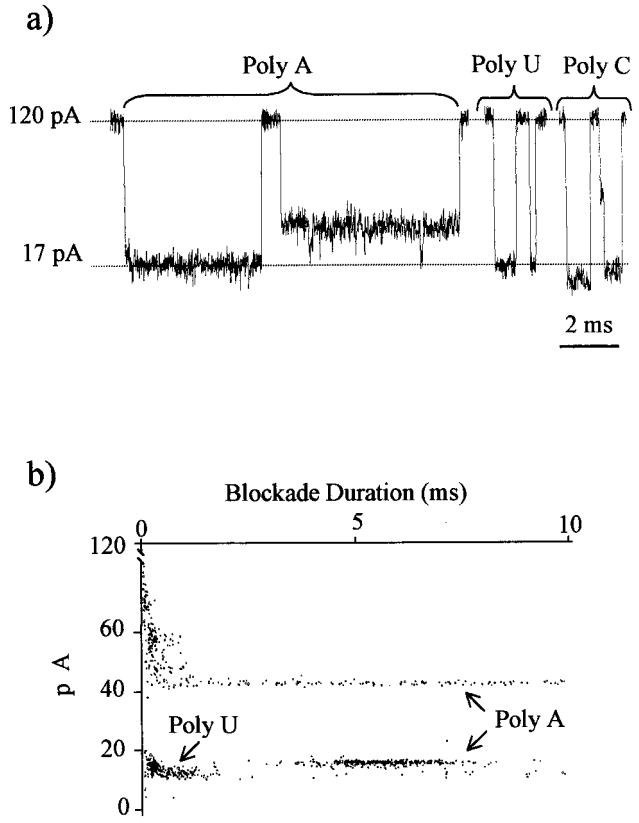

FIGURE 3 Current in the α-hemolysin pore during occupancy by homopolymers of poly A, poly C, or poly U. Data were acquired at 3-μs intervals (100 kHz bandwidth) for 30 s in the presence or absence of 10 μg polynucleotide. The nominal lengths were poly C, 130 $\pm$ 20 nt; poly A, 175 $\pm$ 50 nt; and poly U, 150 $\pm$ 50 nt. Each 30-s acquisition was repeated three times. (*a*) Current traces for poly A, poly C, and poly U. (*b*) Scatter plot in which each point corresponds to the amplitude and duration of a current blockade caused by a single poly U or poly A homopolymer passing through a single α-hemolysin pore. The data in both (*a*) and (*b*) were digitally filtered at 25 kHz bandwidth.

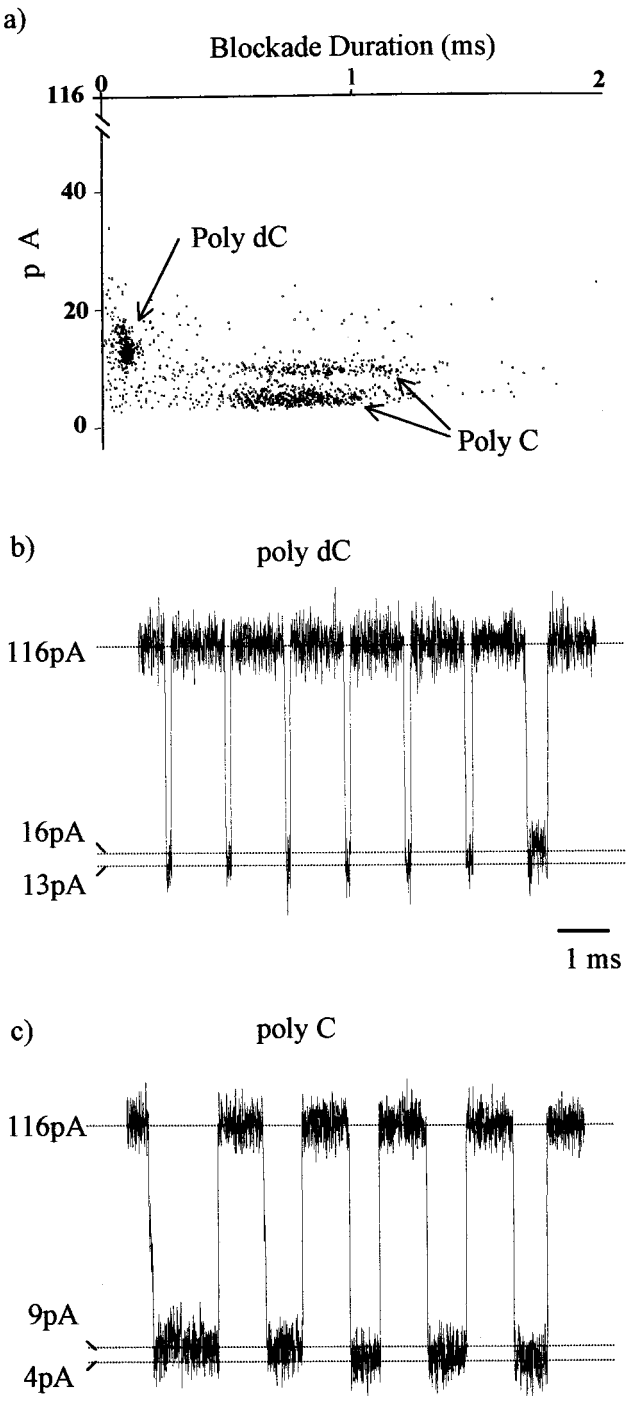

FIGURE 4 Comparison between poly C and poly dC current blockades. The poly C was a 130 $\pm$ 20 nt nominal-length strand purified by PAGE; the poly dC was a synthetic 100-mer purified by PAGE. (*a*) Scatter plot in which each point corresponds to the amplitude and duration of a current blockade caused by a single polynucleotide passing through the α-hemolysin pore. (*b* and *c*) Typical blockades caused by the poly dC and poly C molecules used in (*a*) above. The data in these experiments were digitally filtered at 50 kHz. Quiescent periods between events were spliced out so that numerous blockades could be presented in (*b*) and (*c*).

1964; Sarkar and Tang, 1965; Arnott et al., 1976). The structure of this helix is narrow enough to traverse the pore and could cause greater blockage than an extended chain of pyrimidines.

To test this reasoning, we compared blockade amplitudes from poly C with those from poly dC. Under the same conditions, the helical conformation of single-stranded poly dC is less stable than that of poly C (Adler et al., 1967). If the large blockades caused by poly C were the result of its secondary structure as a helix, the more disordered poly dC would be expected to produce blockades of lesser amplitude. This expectation proved to be correct (Fig. 4). Poly dC 100-mer caused 89% and 86% blockades averaging 100 μs in duration. For the same α-hemolysin channel, poly C (130 $\pm$ 20 nt) caused 95% and 91% blockades averaging 750 μs.

Analysis of RNA block copolymers

The homopolymer data suggested that a transition from poly A to poly C segments within an individual RNA molecule should be detectable by the α-hemolysin pore. We therefore examined blockades caused by RNA of nominal composition $A_{(30)}C_{(70)}Gp$. As expected from the homopolymer data,

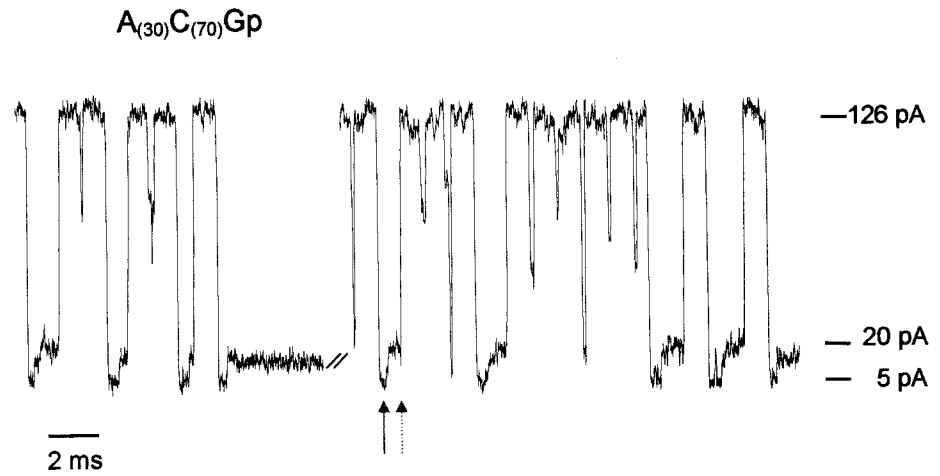

FIGURE 5 Typical blockades of monovalent ion current in the α-hemolysin pore caused by $A_{(30)}C_{(70)}Gp$ RNA. In this and four other similar experiments, most bilevel events first exhibited 5 pA residual current (95% current blockade, *solid arrow*) followed by a 19 pA residual current (85% blockade, *dashed arrow*). Because the 95% blockade is typical of poly C, we interpreted these events as the poly C segment at the 3′ end of the molecule entering the pore first. The opposite orientation constituted <10% of the bilevel blockade events. $A_{(30)}C_{(70)}Gp$ RNA caused frequent permanent blockades of the pore that required voltage reversal to be cleared. These permanent blocks may have been caused by polymer tangles. Quiescent periods between events were spliced out so that numerous blockades could be presented in one figure.

~50% of the polymer-channel interactions produced bilevel blockades. One component of the blockade reduced the channel current by ~95% (consistent with poly C), and the other component reduced the current by ~85% (consistent with poly A) (Fig. 5). We note that the bilevel events were almost exclusively 95% to 85% blockades (Fig. 5). In other words, the 3′ poly C end of $A_{(30)}C_{(70)}Gp$ entered the pore first when a bilevel signature was observed; the opposite orientation (5′ poly A end first) was rare. This asymmetry was consistent with the homopolymer data in Fig. 2, which showed that most of the poly C interactions with the pore led to full 95% blockades that correlated with polymer translocation. In contrast, most of the poly A interactions produced blockades of lesser amplitude that probably represented transient partial entry of polymers into the pore without translocation.

Although these results suggested that purine and pyrimidine segments in single polymers could be detected by the channel, we have observed that a variety of pure DNA or RNA homopolymers occasionally produced similar bilevel blockades. It was therefore important to establish that the bilevel signatures in Fig. 5 specifically arose from the C-to-A transition in $A_{(30)}C_{(70)}Gp$. To test this, we measured blockades caused by $A_{(30)}C_{(70)}Gp$ before and after addition of ribonuclease A. Ribonuclease A cleaves single-stranded RNA on the 3′ end of pyrimidine (but not purine) residues and would therefore be expected to cut the $A_{(30)}C_{(70)}Gp$ into a mixture of truncated $A_{(30)}C_{(n<70)}$ polymers, short poly C homopolymers, and $A_{(30)}C_{(1)}$ polymers. Continued digestion by ribonuclease A would ultimately yield a mixture of $A_{(30)}C_{(1)}$ polymers and cytidylic acid monomers.

The distribution of pore blockades followed the predicted digestion pattern (Fig. 6). Ribonuclease A caused an abrupt decrease in the proportion of bilevel 95%-to-85% blockades accompanied by an increase, then a decrease to near zero of the 95% blockades characteristic of poly C homopolymers. The number of 85% blockades characteristic of poly A increased to a steady-state maximum over the same time period. These results strongly support the conclusion that the α-hemolysin pore can distinguish between poly C and poly A segments within a single RNA molecule.

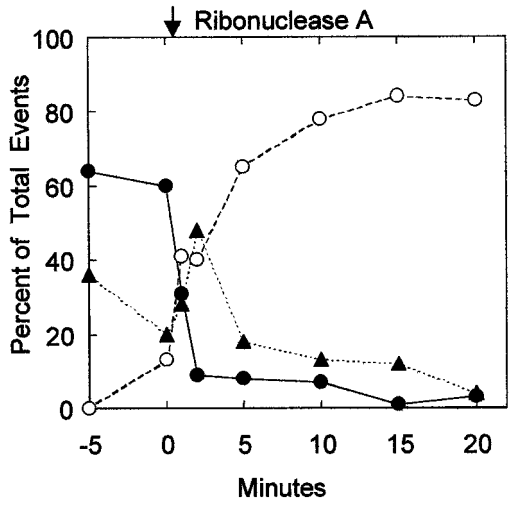

FIGURE 6 Effect of ribonuclease A addition on the frequency of bilevel blockades caused by $A_{(30)}C_{(70)}Gp$ RNA. Three α-hemolysin channels were inserted into the bilayer. After control measurements in the absence of RNA, $A_{(30)}C_{(70)}Gp$ RNA was added to the *cis* bath for a final concentration of 50 μg/ml. Channel blockades were acquired in 1-min increments before RNAase A addition (−5 and 0 min on the time-scale shown). Ribonuclease A (30 $\mu g\ ml^{-1}$) was then added to the *cis* bath (*arrow*), and blockades were acquired in 1-min increments at intervals up to 20 min. (●), C-to-A bilevel blockades; (○), poly A blockades; (▲), poly C blockades.

DISCUSSION

Previous reports have shown that channel conductance can be used to detect the presence of macromolecules in a channel pore (Bezrukov et al., 1994, 1996; Bustamante et al., 1995; Kasianowicz et al., 1996). The evidence presented here demonstrates that single-channel conductance measurements can also be used to analyze the composition and linear sequence of monomers in a single polymer molecule. Thus, individual molecules of poly C, poly A, poly U, and poly dC can be distinguished from each other on the basis of blockade amplitude, blockade time, or both (Figs. 2–4). Furthermore, two segments composed of purine and pyrimidine bases within a single poly $A_{30}C_{70}$ molecule can be distinguished from each other during the polymer's translocation through the α-hemolysin channel (Figs. 5 and 6).

We considered two possible explanations for the unusually large amplitude of the poly C blockade. 1) Cytosine specifically interacts with residues in the α-hemolysin pore to reduce ionic flux more than the other bases. For example, the association constant of cytosine for lysine at room temperature and neutral pH is ~10-fold greater than that of adenosine (Bruskov, 1978). A cytosine-specific interaction with the ring of lysines that forms the limiting aperture within the α-hemolysin pore is therefore plausible. 2) Poly C traverses the channel's pore as a helix, producing a greater obstruction to ionic current than other polymers that traverse in an extended form. The helical structure of poly C is relatively stable at room temperature (Fasman et al., 1964; Sarkar and Tang, 1965, Adler et al., 1968), and x-ray diffraction analysis of poly C fibers (Arnott et al., 1976) implies base-stacking to form an unusually slender, 1.3-nm diameter helix that could fit through the 1.5-nm limiting aperture of the α-hemolysin channel (Song et al., 1996). We favor the second explanation because a specific interaction between cytosine and residues in the α-hemolysin pore cannot account for the significantly greater amplitude of poly C blockades compared with poly dC blockades (Fig. 4). Thus, some other structural feature of poly C must account for its ability to sharply block ionic flow through the α-hemolysin channel. In view of the more stable base-stacking in poly C compared with poly dC (Adler et al., 1967), the simplest assumption is that poly C traverses through the α-hemolysin channel as a helix, whereas poly dC traverses in a disordered and extended state (Fig. 7).

We note that poly C causes two classes of blockades (Figs. 2–4) that are about equal in number and duration but measurably different in amplitude (91% current reduction versus 95% current reduction). This may represent translocation of poly C molecules in either of two different conformations that are in equilibrium with each other, or it may represent translocation of the same structure in either of two orientations, 3′ to 5′ or 5′ to 3′.

Unlike poly C, poly U lacks any ordered local structure that is measurable by hypochromism or by circular dichroism (Cantor and Schimmel, 1980). This is supported by NMR spectroscopy (Evans and Sarma, 1976) and by hydrodynamic data that reveal that poly U at room temperature has the same radius of gyration as poly A at high temperature (Inners and Felsenfeld, 1970). Thus, poly U-induced blockades (Fig. 3 and Kasianowicz et al., 1996) represent capture and translocation of disordered and extended RNA chains (Fig. 7).

As shown in Fig. 3, current blockades induced by individual poly A molecules cannot be distinguished from poly U based on amplitude, but they can be distinguished from poly U based on average blockade duration and the frequent occurrence of a bilevel signature. The long blockade duration characteristic of poly A (average 22 μs/nucleotide) is not consistent with an adenosine-specific effect because poly-deoxyadenylic acid 100-mers traverse the pore at an average rate of 3 μs/nt (Meller et al., manuscript in preparation). We postulate that the slow traversal of poly A is accounted for by its helical structure at room temperature and neutral pH (Holcomb and Tinoco, 1965; Leng and Felsenfeld, 1966; Brahms et al., 1966). But unlike the narrow, 1.3-nm poly C helix, the poly A helix is believed to have a diameter of ~2.1 nm (Saenger et al., 1975), with 7-to-50-nt segments of helix interspersed among unstacked segments. The 2.1-nm diameter is small enough to enter the α-hemolysin vestibule (limiting aperture ~2.6 nm, Song et al., 1996) but too wide to traverse the 1.5-nm limiting aperture in the neck of the α-hemolysin channel (Fig. 7). Thus, helical segments along a poly A strand must be partially unwound and extended to permit translocation through the channel pore. We propose that the stochastic process of unstacking and unwinding poly A accounts for the relatively long and broad spread of poly A traversal times.

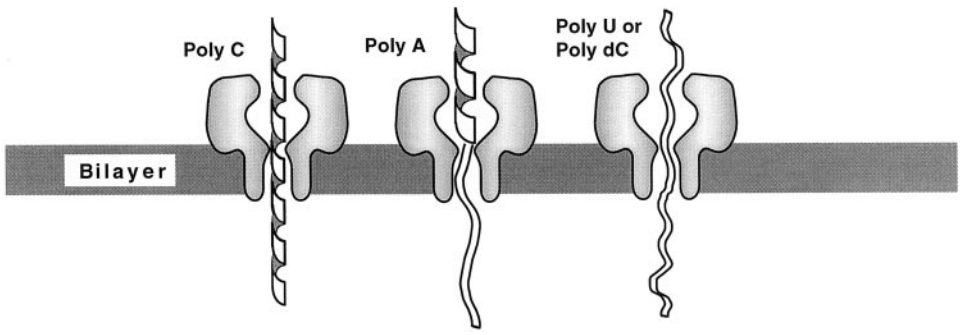

FIGURE 7 Model of RNA homopolymer conformers that are captured and translocated across the α-hemolysin pore.

Although we are greatly encouraged to find that the α-hemolysin nanopore has sufficient sensitivity and resolution to detect a 30-nucleotide segment of poly A attached to a longer poly C segment, we were surprised to discover, as reported here, that the single-stranded helical structures of RNA homopolymers turned out to be major factors in modulating the amplitude of blockade events. It follows that if membrane channels are to provide a direct, high-speed read-out of the sequence of bases in an RNA or DNA polymer, experimental conditions will need to be optimized to distinguish between the individual purine and pyrimidine nucleotides rather than between the stacked structures they tend to form at room temperature. While it will be of interest to investigate blockade amplitude and duration at elevated temperatures, it is apparent that in future nanopore sequencing applications the blockade characteristics produced by an individual nucleotide will have to be read with greater precision than can be achieved at polymer traversal rates exceeding 1 base per 10 μs. Methods to slow traversal time while maintaining a sufficiently high voltage to overcome backward polymer movement are being evaluated. We expect that with such refinements single nucleotide detection may be achievable, thus permitting direct nanopore sequencing of very long individual nucleic acid strands.

We thank Frits Van Dyk for help in manufacturing the planar thin film device.

This work was supported by the National Human Genome Research Institute (Grant HG01826-01) and by Defense Advanced Research Projects Agency.

REFERENCES

Adler, A., L. Grossman, and G. D. Fasman. 1967. Single-stranded oligomers and polymers of cytidylic and 2′-deoxycytidylic acids: comparative optical rotatory studies. *Proc. Natl. Acad. Sci. USA*. 57:423–430.

Adler, A. J., L. Grossman, and G. D. Fasman. 1968. Circular dichroism of cytosine dinucleoside monophosphates containing arabinose, ribose, and deoxyribose. *Biochemistry*. 7:3836–3843.

Arnott, S., R. Chandrasekaran, and A. G. W. Leslie. 1976. Structure of the single-stranded polyribonucleotide polycytidylic acid. *J. Mol. Biol.* 106: 735–748.

Bezrukov, S. M., I. Vodyanoy, R. A. Brutyan, and J. J. Kasianowicz. 1996. Dynamics and free energy of polymers partitioning into a nanoscale pore. *Macromolecules*. 29:8517–8522.

Bezrukov, S. M., I. Vodyanoy, and V. A. Parsegian. 1994. Counting molecules moving through a single ion channel. *Nature*. 370:279–281.

Brahms, J., A. M. Michelson, and K. E. Van Holde. 1966. Adenylate oligomers in single- and double-strand conformation. *J. Mol. Biol.* 15:467–488.

Bruskov, V. 1978. Specificity of interaction of nucleic acid bases with hydrogen bond forming amino acids. *Stud. Biophys. (Berlin)*. 67S: 43–44.

Brutyan, R. A., C. DeMaria, and A. L. Harris. 1995. Horizontal "solvent-free" lipid bimolecular membranes with two-sided access can be formed and facilitate ion channel reconstitution. *Biochim. Biophys. Acta*. 1236: 339–344.

Bustamante, J. O., H. Oberleithner, J. A. Hanover, and A. Liepins. 1995. Patch clamp detection of transcription factor translocation along the nuclear pore complex channel. *J. Membr. Biol.* 146:253–261.

Cantor, C. R., and P. R. Schimmel. 1980. Biophysical Chemistry, Part I: The Conformation of Biological Macromolecules. W. H. Freeman, San Francisco.

Evans, F. E., and R. H. Sarma. 1976. Nucleotide rigidity. *Nature*. 263: 567–572.

Fasman, G. D., C. Lindblow, and L. Grossman. 1964. The helical conformations of polycytidylic acid: studies on the forces involved. *Biochemistry*.3:1015–1021.

Holcomb, D. N., and I. Tinoco, Jr. 1965. Conformation of polyriboadenylic acid: pH and temperature dependence. *Biopolymers*.3:121–133.

Inners, L. D., and G. Felsenfeld. 1970. Conformation of polyribouridylic acid in solution. *J. Mol. Biol.* 50:373–389.

Kasianowicz, J. J., E. Brandin, D. Branton, and D. W. Deamer. 1996. Characterization of individual polynucleotide molecules using a membrane channel. *Proc. Natl. Acad. Sci. USA*. 93:13770–13773.

Leng, M., and G. Felsenfeld. 1966. A study of polyadenylic acid at neutral pH. *J. Mol. Biol*. 15:455–466.

Saenger, W., J. Riecke, and D. Suck. 1975. A structural model for the polyadenylic acid single helix. *J. Mol. Biol.* 93:529–534.

Sarkar, P. K., and J. T. Tang. 1965. Optical activity and the conformation of polyinosinic acid and several other polynucleotide complexes. *Biochemistry*. 4:1238–1244.

Song, L., M. R. Hobaugh, C. Shustak, S. Cheley, H. Bayley, and J. E. Gouaux. 1996. Structure of staphylococcal α-hemolysin, a heptameric transmembrane pore. *Science*. 274:1859–1865.

Wonderlin, W. F., A. Finkel, and R. J. French. 1990. Optimizing planar lipid bilayer single-channel recordings for high resolution with rapid voltage steps. *Biophys. J.* 58:289–297.